Cellulose derivatives-snail slime films: New disposable eco-friendly materials for food packaging

CELLULOSE DERIVATIVES-SNAIL SLIME FILMS: NEW DISPOSABLE ECO-FRIENDLY MATERIALS FOR FOOD PACKAGING

Maria Francesca Di Filippo[1 §], Luisa Stella Dolci[2 §], Letizia Liccardo[1], Adriana Bigi[1], Francesca Bonvicini[3], Giovanna Angela Gentilomi[3], Nadia Passerini[2], Silvia Panzavolta[1*], Beatrice Albertini[2]

[1]Department of Chemistry "G. Ciamician", University of Bologna, Via Selmi 2, 40126, Italy;

[2]Department of Pharmacy and BioTechnology, University of Bologna, Via S. Donato 19/2, 40127, Italy;

[3]Department of Pharmacy and Biotechnology, University of Bologna, Via Massarenti 9, 40138, Italy

§ these Authors equally contributed to this work

*Corresponding author: Silvia Panzavolta

Dipartimento di Chimica "G. Ciamician"
via Selmi 2 40126 Bologna (Italy)
tel +39 051 2099566
fax +39 051 2099456
silvia.panzavolta@unibo.it

ABSTRACT

In recent decades, synthetic plastic polymers have been the most practical and economical solution for packaging applications due to their low cost, availability, excellent optical, mechanical and barrier properties and resistance against water. However, most of the plastics used for packaging are hardly biodegradable. With a view to a circular economy, the aim of this work focused on the development of a new material made of commercial cellulose derivatives (hydroxypropyl methyl cellulose or carboxymethyl cellulose) mixed with snail mucus extracted from Helix Aspersa Muller. Increasing in Snail Mucus content enhances films elongation and adhesion strength while decreasing water vapor permeability. The cellulose-snail mucus based films are highly transparent but, more interestingly, the mucus confers UV-screening effect. In addition, the composite films exhibit

antimicrobial activity against both Gram-positive and Gram-negative bacteria. Furthermore, snail mucus addition to carboxymethyl cellulose strongly decreases films solubility in water. The biodegradation tests indicate that all the films degrade in soil between two and four weeks. The excellent results indicate that these biocomposite films are very good candidate for food packaging.

Keywords: snail slime; food packaging; cellulose films; barrier properties; biodegradable films

INTRODUCTION

Nowadays, imagining a world without synthetic plastics seems impossible, though their large-scale production and their extensive use have only spread since the end of the World War II. In food packaging it is a mandatory requirement to ensure protection from possible contaminants, as well as from moisture, gases, dust, temperature, UV and light radiation, odors and mechanical stresses. Plastic polymers have been the most practical and economical solution for packaging applications due to their low cost, prompt availability, excellent optical, mechanical and barrier properties and resistance against water and grease (Marsh & Bugusu, 2007). Traditional plastic packagings are petroleum-based products, which continuous and massive use will inevitably lead to reduced availability. However, most of the materials used for packaging, mainly designed for immediate disposal, are not biodegradable and their use provokes significant environmental pollution. Biodegradable materials from renewable resources are considered the best answer to the problems caused by the huge use of plastics. The most abundant renewable polymer is cellulose (Ferrer, Pal & Hubbe, 2017), which is biodegradable and non-toxic (Al-Tayyar, Youssef & Al-Hindi, 2020). Indeed, cellulose-based materials are widely employed in the packaging field (Lee, Yam & Piergiovanni, 2008).

53 For example, hydroxypropyl-methylcellulose (HPMC) is a renewable, largely available and non-ionic
54 vegetable derivative, very attractive because of its interesting properties: it is edible, transparent,
55 odorless, tasteless and able to form oil-resistant and water-soluble films. Moreover, the use of
56 HPMC is approved as food additive by the FDA (21 CFR 172.874) and by the EU (European
57 Commission, 2011) and it is also proposed for the preparation of packaging materials (Wrona, Cranb,
58 Nerín & Bigger, 2017), although it also exhibits a high moisture absorption (Bahrami, Mokarram,
59 Khiabani, Ghanbarzadeh & Salehi, 2018). The highly crystalline derivative sodium carboxymethyl
60 cellulose, CMCNa, which is a GRAS (Generally Recognized As Safe) polymer, is also widely used for
61 film formulations (Arslan & Togˇrul, 2005) and as a food stabilizer thanks to its peculiar properties
62 like non-toxicity, biocompatibility, biodegradability and hydrophilicity. As well as HPMC, CMCNa is
63 highly soluble in water and this feature limits their use as film-forming polymers.
64 In fact, to improve the CMCNa water resistance, crosslinking is mandatory: several chemical
65 reactions have been proposed to overcome this problem (Su, Huang, Yuan, Wang & Li, 2010) as well
66 as conjugation of CMC with montmorillonite by means of DOPA formation, as reported by Guo et al
67 (Guo et al., 2019). Incorporation of additives, such as nanoclays, metallic nanoparticles and
68 crosslinkers (Hasheminya, Mokarram, Ghanbarzadeh, Hamishekar & Kafil, 2018; He, Fei & Li, 2019;
69 Kanatt & Makwana, 2020; Liu, Song, Shang, Song & Wang, 2012) have been proposed in order to
70 increase the water barrier permeability, a further drawback of CMC.
71 However, neither CMC nor HPMC exhibit antibacterial properties, which are highly required in
72 applications aimed to food preservation (Moghimi, Aliahmadi & Rafati, 2017). The research on
73 antimicrobial food packaging films has indeed attracted great attention in recent years (Quintavalla
74 & Vicini, 2002) since they can act as effective physical barriers against bacteria invasion and prolong
75 the food shelf life (Appendini & Hotchkiss, 2002). Compared with the nano-antibacterial agents
76 prepared by different inorganic materials, the introduction of natural extract is considered to be

77 safe and friendly to human and environment (Zhao, Wei, Xu & Han, 2020). Up to now, the studies
78 aimed to imbue these materials with antibacterial activity are indeed based on the use of essential
79 oils as additives (Gómez-Estaca, López de Lacey, López-Caballero, Gómez-Guillén & Montero, 2010;
80 Moghimi, Aliahmadi & Rafati, 2017; Muppalla, Kanatt, Chawla & Sharma, 2014).

81 Herein, we propose the introduction of snail mucus as additive in the preparation of HPMC and CMC
82 films with the aim to develop new materials with antimicrobial properties and highly improved
83 water barrier permeability. Moreover, we have recently demonstrated that snail mucus addition to
84 chitosan films not only provides them with antimicrobial activity, but also remarkably improves their
85 water barrier and bioadhesion properties (Di Filippo et al., 2020). In this study we further explore
86 the influence of snail mucus addition on the structural, mechanical, adhesive, barrier and
87 antimicrobial properties, solubility and biodegradability of HPMC and CMC films. To this purpose,
88 we utilized HPMC at two different viscosities and CMCNa to prepare and characterize films at
89 different snail mucus content.
90
91
92 **EXPERIMENTAL PART**
93 ***2. Materials and Methods***
94 Hydroxypropil methyl Cellulose l (HPMC, Methocel E5 and E50, viscosity at 2% in water = 4-6 mPa·s
95 and 40-60 mPa·s, respectively) were kindly supplied by Colorcon (UK). Commercial Carboxymethyl
96 Cellulose sodium salt, (CMCNa Mw = 250 KDa, viscosity at 2% in water= 850 mPa·s) was kindly
97 donated by ACEF (Piacenza, Italy). Formulae are reported in SI, Figure S1. These Celluloses satisfy
98 the standards of the United States Pharmacopeia and European Pharmacopeia. Snail mucus or snail
99 slime (S) from *Helix Aspersa Muller* (kindly offered by "I Poderi" farm, Montemerano, GR, Italy) was
100 extracted by MullerOne method (http://www.mullerone.com/it/en/extraction-process) and stored

101 at 4°C in a sealed polyethylene bottle until use. Analysis of snail mucus was obtained from the
102 supplier and reported in supplementary materials (Table S1).

103 ***2.1 Preparation of cellulose films***

104 Cellulose films were obtained by solvent casting. Films forming solutions were prepared by
105 dissolving 1 g of E5 or E50 in 20 mL of distilled water (5% w/v) or 0.4 g of CMC in 20 mL of distilled
106 water (2% w/v) under gently stirring overnight. Then, 10.2 g of this solutions were poured in
107 polyethylene Petri dishes (Ø= 8.5 cm) and allowed to dry under a laminar hood at room temperature
108 overnight. The obtained films were labeled E5, E50 and CMC respectively and stored at room
109 temperature between two sheets of plastic-coated aluminum closed inside PVC bags.

110 ***2.2 Preparation of cellulose films with snail mucus extract***

111 In order to obtain films based on E5, E50 and CMC containing different amounts of snail mucus (S)
112 (30, 70 and 100 % v/v), the relative volume of S was added to the solution containing 1 g of HPMC
113 or 0.4 g of CMC, previously dissolved in the remaining volume of water. When S is at 100%, the
114 polymer is directly solubilized into the snail mucus. After complete dissolution and disappearance
115 of bubbles, 10.2 g of this solution were poured in each Petri dish (Ø= 8.5 cm) and put under laminar
116 flow hood overnight. The obtained films were labeled as reported in Table 1, according to the
117 volume of S used.

118 Table 1. Film compositions and labels.

Label	Polymer type	Polymer % (w/v)	S % (v/v)	Water % (v/v)
E5	HPMC E5	5	0	100
E5_S30	HPMC E5	5	30	70
E5_S70	HPMC E5	5	70	30
E5_S100	HPMC E5	5	100	0
E50	HPMC E50	5	0	100
E50_S30	HPMC E50	5	30	70
E50_S70	HPMC E50	5	70	30
E50_S100	HPMC E50	5	100	0
CMC	CMC Na	2	0	100
CMC_S30*	CMC Na	2	30	70

CMC _S70	CMC Na	2	70	30
CMC _S100	CMC Na	2	100	0

*Due to their excessive fragility, it was not possible to characterize the films corresponding to the composition CMC_S30.

2.3. Films Characterization

2.3.1 Thickness

The thickness of the films was measured with a hand-held digital micrometer (Mitutoyo, Japan) to an accuracy of 0.001 mm.

2.3.2 Tensile tests

Tensile tests were performed on the samples immediately after drying using a 4465 Instron dynamometer equipped with a 100 N load cell and the Series IX software package. Stress-strain curves were recorded at a crosshead speed of 5 mm/min on strip-shaped samples (20-30 mm long and 4 mm width). The Young's modulus (E), the stress at break (σ_b) and the strain at break (ε_b) were evaluated. At least 10 samples were tested for each composition and the mean ± SD are reported.

2.3.3 Structural Characterization

Fourier transform infrared spectra were recorded using a Thermo Scientific Nicolet iS10 FTIR spectrometer equipped with an ATR sampling device, using a Germanium crystal as internal reflection element. Infrared spectra were acquired at room temperature in absorbance mode from 4000 to 800 cm^{-1} with a resolution of 2 cm^{-1}.

X-ray diffraction patterns were recorded using a Philips X'Celerator diffractometer equipped with a graphite monochromator in the diffracted beam. CuKα radiation (40 mA, 40 kV, 1.54 Å) was used. The 2θ range was from 4° to 40°with a step size of 0,1337° and time/step of 40s.

2.3.4 Tack test

The adhesive strength of the films was evaluated by means of Antoon Paar modular compact Rheometer MCR102 with the Rheo Compass software, adapting the method reported in literature (Duncan, Abbott & Roberts, 1999). Glass and aluminum supports were used for the test. Films were cut in 3 cm-diameter circles and allowed to adhere to the two different supports by wetting them with 10 µL of distilled water and applying a gentle finger pressure. The upper plunger of the instrument was covered with double-sided tape (3M) and was lowered until a force of 5 N was applied to the film. After 30 seconds, the plunger was raised up at a speed of 1 mm/s, collecting the peak detachment force and the work of adhesion of the film from the support. Each formulation was analyzed in triplicate and the mean ± SD was reported.

2.3.5 Barrier properties

Water Vapor Permeability (WVP)

WVP is the water vapor transmission rate through a flat film area induced by a vapor pressure between two surfaces under specific conditions of moisture and temperature and was measured using the ASTM E96-93 method (ASTM, 1993), slightly modified as reported in literature (Bozdemir & Tutas, 2003).

Films circles (2 cm-diameter) were glued with silicon on the opening of glass vials containing 2 g of anhydrous $CaCl_2$. Vials were weighted and placed in a glass desiccator containing saturated $Mg(NO_3)_2 \cdot 6H_20$ solution (75% RH at 25°C). The vials were weighted every day until constant weights were achieved. WVP was calculated as follows:

$$WVP\ (gs^{-1}m^{-1}Pa^{-1}) = \Delta W\ \chi\ /\Delta t\ A\ \Delta P \quad (1)$$

where $\Delta W/\Delta t$ is the amount of water gained per unit time of transfer, A is the exposed area of the samples (0.00020 m^2), ΔP is water vapor pressure difference between both sides of the film (1670 Pa at 25°C, table value) and χ is the film thickness. Samples were tested in triplicate.

Moisture sorption

166 The weighed films were placed inside glass dryers at room temperature containing different
167 saturated solutions, thus providing different environments with constant relative humidity (RH)
168 between 38 and 98%. Samples were weighed after predetermined periods of time until 3 different
169 consecutive measures gave the same results. The moisture content at equilibrium was calculated
170 on dry samples, preconditioned in stove at 40°C, from which the final isotherms were obtained
171 (Bajpai, Chand, & Chaurasia, 2010).

172 ***2.3.6 Film solubilization and swelling ability***

173 Square- shaped (1cm×1cm) cellulose films were weighted and immersed into 5 mL of distilled water.
174 After predetermined periods of time, ranging from 2 minutes to 24 hours, wet samples were
175 removed from water, wiped with filter paper to absorb excess liquid, weighted and put into water
176 again. The extent of swelling was calculated as follows:

177 $$\text{Swelling (\%)} = \frac{Ww - Wd}{Wd} \cdot 100 \qquad (2)$$

178 where Ww and Wd are the weights of the wet and the air-dried sample, respectively.
179 After 24 hours the samples not completely dissolved were removed from water and dried until a
180 constant weight was obtained. Solubilization as a consequence of the water uptake and dissolution
181 of the film, as reported by Hosseini et al, (Hosseini, Rezaei, Zandi & Farahmandghavi, 2015) was
182 calculated as follows:

183 $$\text{Solubilization (\%)} = \frac{Wi - Wf}{Wi} \cdot 100 \qquad (3)$$

184 Solubility tests at longer times (7 and 14 days) were performed in the same way only on the samples
185 not completely dissolved after 24 hours.

186 ***2.3.7 UV-Vis Spectroscopy***

187 In order to evaluate the barrier properties of the films against UV-Vis light, films were cut into 1 cm
188 wide rectangular strips, which were inserted into the sample holder of the Cary 60 Uv-Vis

spectrophotometer. Spectra were acquired in transmittance mode from 200 to 800 nm. The transparency of the films was evaluated from transmittance at 600 nm, by the following equation

$$\text{Transparency} = \frac{-\log T_{600}}{X} \quad (4)$$

where T_{600} is the fractional transmittance at 600 nm and X is the thickness of the film (mm). The analysis were done in triplicate.

2.3.8 Antibacterial tests

Cellulose-based films were tested *in vitro* for the evaluation of antibacterial activity by a standardized Kirby-Bauer (KB) diffusion test on Mueller-Hinton agar plate (EUCAST, 2016). For the analysis, a panel of Gram positive and Gram negative reference bacterial strains were selected: *Staphylococcus aureus* (ATCC 25923), *Staphylococcus epidermidis* (ATCC 12228), *Enterococcus faecalis* (ATCC 29212), *Escherichia coli* (ATCC 25922), *Pseudomonas aeruginosa* (ATCC 27853), and *Klebsiella pneumoniae* (ATCC 9591). The effectiveness of the disk-shaped cellulose films (Ø= 6 mm) to inhibit bacterial growth was determined by measuring the diameter of the bacterial-free zone around the sample after 24 hours of incubation at 37°C. In compliance with the International guidance documents in susceptibility testing, disks containing gentamicin (GMN 10 µg) and/or imipenem (IPM 10 µg) (Oxoid SpA, Italy) were included as reference controls (CLSI, 2015). All experiments were performed in duplicate and in different days.

2.3.9 *Biodegradation test*

Biodegradation tests of cellulose films were conducted in soil referring to the literature (Zhao, Lyu, Lee, Cui, & Chem, 2019). Soil was taken from the surface layer in the garden then put in a plastic tray to a thickness of around 4 cm. The films were cut into small pieces (about 2×2cm^2), dried at 37°C until a constant weight was raised and then buried about 2 cm beneath soil. The average of the temperature was about 25 °C. Water was sprayed once on the soil surface to maintain the

moisture. The degraded samples and fragments were taken out after 2 and 4 weeks, gently cleaned from residual soil with distilled water and dried at 37°C until a constant weight was obtained. Finally, the dried samples were weighted again and the weight loss of the film degraded in soil was calculated.

2.3.10 Statistical analysis

Statistical analysis was performed with Graph Pad Prism 4. One-way analysis of variance (ANOVA) followed by Tukey's Multiple Comparison Test was employed to assess statistical significance of the experimental conditions for Tensile Tests, Water Vapor Permeability and Adhesive strength. Statistically significant differences were determined at $p<0.05$.

3. RESULTS AND DISCUSSION

3.1 Dissolution behaviour and swelling ability of films

Solubilization and swelling degree measurements are of particular relevance in order to evaluate the films stability in aqueous solutions: in fact, a good resistance is needed when films are proposed for applications such as food packaging (Al-Tayyar, Youssef & Al-Hindi, 2020).

The results of water solubility test show that HPMC-based films are highly soluble and their solubilization in water is immediate, whatever their composition. CMC-based films display a different and more interesting trend: while in absence of snail extract the films solubilize in few minutes, CMC_S70 and CMC_S100 films preserve their structure for more than two weeks. In fact, after 24 hours their solubilization (calculated from Eq. 3) accounted for 30% and 45%, respectively, and these values are unchanged even after 7 and 14 days, suggesting a good resistance of the films in aqueous solution.

Moreover, both the samples reached a degree of swelling of 100% after 4 hours, with no further significant variation up to 24 hours. These results suggest that the interactions between HPMC and the snail slime are not strong enough to build a network resisting to water permeation, which resulted in an increase of the free volume in the material structure (Bertuzzi, Armada & Gottifredi, 2007).

On the contrary, the significant decrease of the dissolution of the CMC-based films with the addition of S leads to hypothesize that the protonation of the COO^- groups into COOH could occurs due to acidic pH, as reported in literature (Qiu, Shaoa, Liuc, Wanga, Lic & Zhao 2014). Since CMC is less soluble than CMC sodium salt the occurrence of this transformation might account for the reduced solubility of CMC_S70 and CMC_S100.

3.2 Structural characterization

The infrared spectra collected from E5 and E50 are reported in Figure 1 a,b. The characteristic absorption bands of HPMC, in accordance with those reported in literature (Ding, Zhang & Li, 2015), can be detected: in particular, the absorption bands at 3500 cm^{-1}, 1060 cm^{-1} and around 2915 cm^{-1} are due to O-H, C-O and C-H stretching vibration, respectively, whereas the absorption band around 1457 cm^{-1} is characteristic of the CH_3 asymmetric bending vibrations. S addition provokes the appearance of new bands, centered at 1717, 1390 and 1224 cm^{-1}, which can be attributed to the high amount of Allantoin and glycolic acid contained into Snail Mucus extract (see Table S1 and Figure S2).

In the FTIR spectra collected from CMC-based films (Figure 1c) the bands belongings to the functional groups of CMC are well recognizable: the O-H stretching and bending vibrations occur at 3385 cm^{-1} and 1324 cm^{-1}, respectively, while antisymmetric and symmetric vibrations bands of –COO- are at 1600 and 1413 cm^{-1}. The absorption band at 1059 cm^{-1} arises from the asymmetric stretching of glycosidic bridge C-O-C. The low intensity band centered at around 900 cm^{-1} could be

attributed to the β- glycosidic linkages between sugar units (Tong, Xiao & Lim, 2008). As observed for HPMC-based films, introduction of snail extract into CMC-based films strongly modifies the IR spectra, which in addition display an impressive broadening. Figure 1c clearly shows the strong reduction of the intensity of the band at 1593 cm^{-1} (attributable to the asymmetric stretching vibration of free carboxyl groups in the salt form), and the appearance of two bands at 1717 and 1224 cm^{-1} as a consequence of S addition. The band at 1717 cm^{-1} could be due both to S addition (as stated above) and to the formation of COOH groups on the side chain of CMC, as a consequence of pH lowering. The reduction of the charge on the side chains supports the strong effect observed on the swelling properties and on the water uptake ability of CMC_S70 and CMC_S100, as well as the decrease in solubility.

The X-ray patterns recorded on cellulose-based films are reported in Figure 2a-c. It is known that crystallinity of cellulose is associated with strong hydrogen bonding interaction of cellulose (intermolecular and intramolecular) and Van der Waals forces between adjacent molecules. During the processing of cellulose, reactions of methylation and carboxymethylation result in the extending the distance between cellulose molecules, thus disrupting hydrogen bonds and hence lowering the crystallinity of the polymers (Sunardi, & Ahmad 2017). As a matter of fact, the reference films show the characteristic diffraction patterns of a poorly crystalline material, with two broad reflections at 9.5-12°/2theta and 20.0-21.5°/2theta characteristic of cellulose II (Kamide et al., 1985), which is obtained by means of chemical and physical treatments of Cellulose I, the most abundant form found in nature (O'sullivan, 1997; Pérez & Mazeau, 2005).

The broadness of the reflections increases on increasing slime content, in agreement with a decrease of crystallinity. This effect, even more evident in the patterns of CMC films where the signal between 9.5 and 12°/ of 2theta is no longer appreciable, might be attributable to the presence of S interlaid between the polymer chains.

283 ***3.3 Barrier properties***

284 The barrier properties of a polymeric film are crucial features to predict the behaviour of the
285 material as well as the shelf-life of the product when used as a food packaging (Siracusa, Rocculi,
286 Romani & Rosa, 2008) and they derive mainly from the permeability of the film to gases and vapors,
287 that are noxious to the quality of the product (Zeman & Kubìk, 2007).

288 The thickness measurements of the films are reported in Table 2: thickness ranged from 29 to 171
289 microns. For every type of cellulose, the thickness increased on increasing the S amount. As all the
290 films were prepared by casting the same amount of solution into Petri dishes with 8.5 cm in
291 diameter, the observed trend could be due to the increasing of the dry matter. In fact, the snail
292 extract contains approximately a 5% w/v of dry matter, and so, on increasing the S content the total
293 amount of dry matter also increases and the thickness is greater. As thickness influences mechanical
294 and barrier properties, all the values are normalized with respect to thickness.

295 **Water Vapor Permeability (WVP)**

296 Prevention of moisture transfer between food and the surrounding atmosphere or between two
297 different food products is a main requirement of packaging films (Bajpai, Chand, & Chaurasia, 2010).
298 Water vapor permeability (WVP) was used to test whether moisture can easily penetrate and pass
299 through a substance and the results for the different film compositions are reported in Figure 3.
300 The data show that the introduction of snail extract into film composition strongly influences the
301 WVP, which decreases by one or two orders of magnitude as a function of S content: for example,
302 the WVP values vary from $1.3 \cdot 10^{-10}$ to $6.5 \cdot 10^{-12}$ g·m/s·m^2·Pa when measured on E5 and E5_S100,
303 respectively.
304 This trend could be explained by the formation of a polymeric network within the films: the different
305 internal structure could lead to the creation of fewer empty spaces, preventing or hindering the
306 diffusion of water molecules through the films. Greater S contents (S70 and S100) provoke a greater

barrier effect, independently from the HPMC molecular weight (E5 and E50). In addition, the decrease in WVP of CMC-based films could also be due to a decrease in the hydrophilicity and solubility of the films as the Solution content increases (Muppalla, Kanatt, Chawla & Sharma, 2014).

Moisture sorption

The water sorption isotherm represents the relationship between equilibrium moisture content and water activity at a given temperature and it is the major tool to describe and predict the water mobility in the films at different environments (Cazon, Velazquez & Vàzquez, 2020). Water sorption isotherms of HPMC based films (see Figure S3 a) showed an initial slight increase in moisture content at lower RH values, while a rapid increase in superficial water adsorption was observed at RH values higher than 60%, a typical behaviour of hydrophilic materials (Enrione, Hill & Mitchell, 2007; Gontard, Guilbert & Cuq, 1993; Villalobos, Hernández-Muñoz & Chiralt, 2006).

For HPMC films (E5 and E50) the snail slime addition implies an increase in the moisture absorption, which could be due to the creation of additional hydrogen bonds between the exposed groups on the surface and the water molecules (Enrione, Hill & Mitchell, 2007). The increasing of moisture adsorption matched the increasing and broadening of the band centered at about 3400 cm^{-1} in the infrared spectra reported in Figure 1 a-b.

On the other hand, the observed decrease in the moisture absorption of CMC films on increasing S content (see Figure S3 b) suggests that the formation of an insoluble network reduces the number of the surface groups which can form hydrogen bond.

UV barrier, light transmittance and transparency value

Transparency of films for food packaging applications is one of the main requirements in the packaging industry (Haghighi et al., 2019a), as well as the UV barrier properties are a key feature to prevent chemical reactions induced by UV light in food (Wu, Sun, Guo, Ge & Zhang, 2017). In fact, the UV-radiations are responsible for the activation of reactions such as lipid oxidation, vitamins

oxidation or loss of colour which result in a loss of the quality of packaged foods (Guo, Ge, Li, Mu & Li, 2014). However, the mechanisms that allow films to acquire the UV light barrier properties can affect their transparency. The spectra acquired in transmittance mode on the cellulose-based films in the UV-visible region are shown in Figure 4. In the UV region (200-280 nm) samples E5, E50 and CMC show high transmittance values (see Figure 4a, 4b and 4c, respectively), which rapidly fall to zero after S addition. As reported in literature (Haghighi et al., 2019b), a transmittance value below 10% at 280 nm indicates that the films have effective UV barrier properties. It can be concluded that S addition confers excellent UV barrier properties both to HPMC and CMC based films (see Figure 4 a-c), regardless the S content.

By comparing spectra in figure 4 a-c it is worth of note that S-containing films showed also a lower transmittance in the visible range (400–800 nm) than the control films, indicating that the incorporation of snail extract into the film composition had a strong effect on the barrier properties also against visible ligth. A quantitative evaluation of this important feature is obtained by using equation 4 and the obtained transparency values are reported in Table 2. According to this value, the greater is the transparency value the lower is the transparency of the film (Nur Hazirah, Isa & Sarbon, 2016, Guo et al. 2014, Theerawitayaart, Prodpran, Benjakul, & Sookchoo, 2019). For E50 and CMC based films, the transparency decreases on increasing the amount of S, while S addition has a minor effect on E5-based films. Anyway, all the transparency values are lower than 5, and hence the films can be considered transparent, as reported in literature. The mechanism of action of the snail mucus could be due to the combination of two elements: the absorption of UV rays thanks to the presence of proteins containing aromatic amino acids and the decrease in transparency that prevents the visible light passing through the films (Hamaguchi, WuYin & Tanaka, 2007) that can be attributed to the effect of the macromolecular components of S dispersed into the biopolymers

matrix, which could change the optical properties of the material. This effect is more pronounced for E50 and CMC -based films probably due to the higher viscosity of these solutions.

Table 2. Thicknesses and transparency values of the obtained cellulose-based films.

Labels	Thickness (µm)	$T_{600}/100$	Transparency Values
E5	84	0.90	0.545
E5_S30	113	0.87	0.535
E5_S70	158	0.85	0.447
E5_S100	171	0.84	0.443
E50	59	0.90	0.776
E50_S30	85	0.76	1.402
E50_S70	126	0.65	1.485
E50_S100	137	0.50	2.197
CMC	29	0.92	1.249
CMC _S70	60	0.77	1.892
CMC _S100	91	0.40	4.373

3.4 Mechanical properties

The tensile strength at break (σ_b), the elastic modulus (E) and the deformation at break (ε_b) are reported in Table 3, while the stress-strain curves are shown in Figure 5.

Table 3. Effect of S incorporation on thicknesses and tensile properties of cellulose -based films.

Labels	σ_b *(MPa)*	ε_b *(%)*	*E (MPa)*
E5	50 ± 6	16 ± 8	1760 ± 400
E5_S30	31 ± 3**	13 ± 5	1220 ± 90
E5_S70	18 ± 1***	11 ± 3	720 ± 100**
E5_S100	3 ± 1***	61 ± 8***	72 ± 10***
E50	54 ± 10	22 ± 7	2020 ± 140
E50_S30	49 ± 10	16 ± 7	1920 ± 430
E50_S70	31 ± 3*	34 ± 5	860 ± 80**
E50_S100	13 ± 1***	46 ± 1**	140 ± 20***
CMC	32 ± 4	2 ± 1	2750 ± 600
CMC _S70	5 ± 1***	29 ± 3***	44 ± 14***
CMC _S100	2.7 ± 0.3***	67 ± 6***	2 ± 1***

Each value is the mean of ten determinations and is reported with its standard deviation.
(*p < 0,05; **p < 0,01; ***p < 0,001 compared to the control)

Both HPMC and CMC films exhibit a high stress at break but they can be extended only by few units percent. Enrichment of the formulation by S addition greatly enhances films extensibilty, whereas it reduces the stress at break and the elastic modulus. Furthermore, the different series of films display different mechanical behavior upon S addition as shown by the stress-strain curves reported in Figure 5: in particular, while E50_S100 and CMC_S100 show an elastic behavior, E5_S100 seems to display a plastic behavior.

The effect produced by S addition to cellulose-based films is similar to that obtained on S-containing chitosan films (Di Filippo et al., 2020): probably, as a consequence of the interactions between S and the polymer chains, the intermolecular interactions between cellulose molecules are reduced, thus facilitating their sliding and improving their mobility.

According to conventional standard (Hosseini et al., 2015; Kim, Lee & Park, 1995), the tensile strength of packaging films must be higher than 3.5 MPa: in this study, all the prepared films, except E5_S100 and CMC_S100, meet this requirement.

3.5 Adhesion studies

As reported in literature for chitosan-based films (Di Filippo et al., 2020), also cellulose-based films become sticky after the S addition: the adhesive properties, expressed in terms of force needed for film detachment (F), are reported in Figure 6. In order to evaluate a possible application of our films in the field of food packaging, adhesive studies were conducted by using aluminum and glass as support: these materials are in fact very used as domestic food container.

Cellulose-based films exhibit good adhesive performances on both the substrates, even if some differences should be remarked. In particular, the adhesion force on glass support shows a fairly linear trend on increasing the amount of S. Furthermore, films based on HPMC E5 are stickier than the others even without S, although its addition considerably increases this property. On the other

391 hand, CMC based films are not very sticky on glass, but the addition of S surprisingly increases the
392 adhesiveness of almost 10 units.

393 **3.6 Preservation of apple cubes.**

394 The effectiveness of the obtained films to preserve the freshness of food and to remain attached to
395 the container for a desirable period of time was qualitatively assessed using a fresh apple purchased
396 in a local shop at commercial maturity and immediately used, following a method reported in
397 literature suitably modified (Shyu, Chen, Chiang & Sung, 2008).
398 The apple was cut into cubes of regular dimensions (side about 1 cm) and arranged into a glass
399 container. The container was covered with the film CMC, as shown in Figure 7, and then placed in
400 the refrigerator at 4°C. As a control, apples cubes were maintained in the refrigerator without any
401 coverage. Digital photos were acquired at time zero and after ten days of storage. After ten days of
402 storage at 4°C, the uncovered apple cubes became dried and darker while those covered with the
403 film showed an excellent state of preservation, allowing only a slight enzymatic browning on their
404 surface (see Figure 7) thus demonstrating the efficacy of CMC_S70 in the preservation of food.
405 Moreover, it is important to underline that the film is able to immediately adhere to the glass
406 container and to remain attached to it for the whole time of storage.
407 A further investigation was made by cutting a small slice of apple and wrapping it with the CMC_S70
408 film in order to check its appearance after ten days of storage in the refrigerator at 4°C.
409 The adhesiveness of the CMC_S70 film on itself and on the surface of an apple together with its
410 effectiveness in food preservation was evaluated from a qualitative point of view. In fact, from the
411 comparison of the digital photos of the apple slice wrapped with CMC-_S70 taken at time zero and
412 after ten days of storage in the refrigerator at 4°C (Figure 8 a,b) no significant oxidative processes
413 have damaged the state of apple conservation.
414

3.7 Antibacterial tests

The antibacterial activity of the different cellulose-based films was assessed *in vitro* by means of a disk agar diffusion method against both Gram positive and Gram-negative bacteria. Results are reported in Figure 9 a,b.

All cellulose films without S did not show any inhibition on the tested bacteria. However, the antimicrobial activity of S containing films on contact surface around the discs was evident, indicating the antibacterial effect of snail mucus. This is further confirmed by the increased diameter of the bacterial-free zone for the samples at the highest S content. Disks used for antibacterial assay were weighted and the S content of each composition was determined, taking into account they contain about 6% wt of residual water. Considering the weight of the cellulose-based films, and the amount of snail mucus on the different 6 mm-diameter disks, it is evident that the inhibitory activity of the samples is strictly related to S content, as reported in figure 10.

Of note, even the cellulose-based disks containing S at 30% displayed a significant inhibitory zone for *Pseudomonas aeruginosa*, one of the most versatile pathogen that is present in a variety of environments, including soil and water, and intrinsically resistant to numerous antibacterial agents. It is an opportunistic pathogen responsible for a broad spectrum of infections as respiratory tract and urinary infections, primary skin infections, ear and eye infections.

3.8 Biodegradability test

Biodegradation tests were conducted in soil, as described in the experimental part. After 2 weeks, only fragments of the sample CMC_S70 were still present: a weight loss of 54% was calculated. After 4 weeks, sample CMC_S70 was fully biodegraded. The biodegradation data meet very well to the results reported in literature (Zhao, Lyu, Lee, Cui, & Chem, 2019) and represent an added value of the snail-containing cellulose films.

4. **CONCLUSIONS**

The results of this work demonstrate that the use of snail mucus extract in the preparation of cellulose derivatives-based films provides materials characterized by high transparency, excellent UV barrier properties and very good WVP. Addition of the snail slime results in an increase of the extensibilty, together with a decrease of the stress at break and of the elastic modulus, in all the three different types of cellulose (HPCM E5, HPCM E50 and CMCNa) films. Moreover, all the films prepared in the presence of S display enhanced adhesion towards glass and aluminum and a significant antibacterial activity against both Gram positive and Gram-negative bacteria.

However, the structural characterization evidenced that the snail extract establishes different interactions with the internal structures of the different types of celluloses. In fact, while immersion in water causes immediate solubilization of all HCPM based films, the addition of high amounts of S to the composition of CMC-based films makes them insoluble for more than a week, thus allowing their use for food packaging. In addition, all the prepared films are fully biodegradable in few weeks. On the basis of these results, it can be inferred that snail-enriched CMC based films might find potential applications that require direct contact with food and they are good candidates to replace synthetic polymers in the packaging industry.

.

This research did not receive any specific grant from funding agencies in the public, commercial, or not-for-profit sectors

CAPTION TO THE FIGURES

Figure 1. Infrared spectra of cellulose-based films containing different amount of S: a) E5_based films; b) E50-based films; c) CMC-based films. The arrows indicate the most intense bands due to S.

Figure 2. X-rays diffraction patterns of cellulose-based films containing different amount of S: a) E5_based films; b) E50-based films; c) CMC-based films.

Figure 3. Water Vapor Permeability of cellulose-based films (***p < 0.001).

Figure 4. UV-Vis spectra collected on cellulose-based films containing different amount of S: a) E5-based films; b) E50-based films; c) CMC-based films. Photographs of (from left to right): E5_100, E50_100 and CMC_100 films.

Figure 5. Stress-strain curves of films obtained by mixing different amount of S with: a) E5, b) E50 and c) CMCNa.

Figure 6. Detachment forces (N) of films from glass and aluminum supports (*p < 0,05; **p < 0,01).

Figure 7: Apple cubes covered with the film CMC_S70 (left) and uncovered (right), at time 0 and after ten days of storage at 4°C.

Figure 8. Apple slice wrapped with the CMC_S70 film a) immediately after cutting and b) after ten days of storage at 4°C.

Figure 9. Antibacterial activity of cellulose-based disks against: a) Gram-positive bacteria; b) Gram-negative bacteria. Data are the mean value of the diameter (in mm) of the clear bacterial free-zone measured around the disk samples.

Figure 10. Antimicrobial activity of the cellulose-based films. Each dot plot is the bacterial-free zone (in mm) measured around the 6 mm diameter disks, for the six reference strains tested in different independent assays. Horizontal lines indicate the median values. S content (in mg) is obtained

considering the weight of the film samples and the amount of snail mucus used for their preparation.

REFERENCES

(Al-Tayyar, Youssef & Al-Hindi, 2020)
Al-Tayyar, N. A., Youssef, A. M., Al-Hindi, R. (2020).
Antimicrobial food packaging based on sustainable Bio-based materials for reducing foodborne Pathogens: A review.
Food Chemistry, 310, 125915.
https://doi.org/10.1016/j.foodchem.2019.125915

(Appendini & Hotchkiss, 2002)
Appendini, P. & Hotchkiss, J.H. (2002)
Review of antimicrobial food packaging.
Innovative Food Science & Emerging Technologies, 3, pp. 113–126.
https://doi.org/10.1016/S1466-8564(02)00012-7

(Arslan & Togˇrul, 2005)
Arslan, N. & Togˇrul, H. (2005)
Modelling of water sorption isotherms of macaroni stored in a chamber under controlled humidity and thermodynamic approach.
Journal of Food Engineering, 69(2), pp. 133-145.
https://doi.org/10.1016/j.jfoodeng.2004.08.004

(ASTM, 1993)
American Society for Testing and Materials (1993)
E96-93 Standard test methods for water-vapor transmission of materials.
Annual Book of ASTM Standards, Philadelphia: American Society for Testing and Materials, 4(6), pp. 701-708.

(Azeredo, Rosa & Mattoso, 2017)
Azeredoa, H. M. C., Rosaa, M. F. & Mattoso, L. H. C. (2017)
Nanocellulose in bio-based food packaging applications.
Industrial Crops and Products, 97, pp. 664–671.
https://doi.org/10.1016/j.indcrop.2016.03.013

(Bahrami, Mokarram, Khiabani, Ghanbarzadeh & Salehi, 2018)
Bahrami, A., Mokarram, R. R., Khiabani, M. S., Ghanbarzadeh, B., & Salehi, R. (2018).
Physico-mechanical and antimicrobial properties of tragacanth/hydroxypropyl methylcellulose/beeswax edible films reinforced with silver nanoparticles.
International Journal of Biological Macromolecules, 129, 1103–1112.
https://doi.org/10.1016/j.ijbiomac.2018.09.045

(Bajpai, Chand, & Chaurasia, 2010)
Bajpai, S. K., Chand, N., & Chaurasia, V. (2010)
Investigation of water vapor permeability and antimicrobial property of zinc oxide nanoparticles-loaded chitosan-based edible film.
Journal of Applied Polymer Science, 115(2), pp. 674-683.
https://doi.org/ 10.1002/app.30550

(Bertuzzi, Armada & Gottifredi, 2007)
Bertuzzi, M. A., Armada, M., & Gottifredi, J. C. (2007).
Physicochemical characterization of starch based films.
Journal of Food Engineering, 82(1), 17–25.
https://doi.org/ 10.1016/j.jfoodeng.2006.12.016.

(Bozdemir & Tutas, 2003)
Bozdemir, O. A. & Tutas, M. (2003)
Plasticiser effect on water vapour permeability properties of locust bean gum based edible film.
Turkish Journal of Chemistry, 27(6), pp. 773-782.

(CLSI, 2015)
Clinical and Laboratory Standards Institute, (2015)
Performance Standards for Antimicrobial Susceptibility Testing.
Twenty-fifth Informational Supplement, CLSI document M100-S25

(Di Filippo et al., 2020)
Di Filippo, M. F., Panzavolta, S., Albertini, B., Bonvicini, F., Gentilomi, G. A., Orlacchio, R., Passerini, N., Bigi, A. & Dolci, L. S. (2020)
Functional properties of chitosan films modified by snail mucus extract.
International Journal of Biological Macromolecules, 143, pp. 126–135.
https://doi.org/10.1016/j.ijbiomac.2019.11.230

(Ding, Zhang & Li, 2015)
Ding, C., Zhang, M. & Li, G. (2015)
Preparation and characterization of collagen/hydroxypropyl methylcellulose (HPMC) blend film.
Carbohydrate Polymers, 119, pp. 194–201.
https://doi.org/10.1016/j.carbpol.2014.11.057

(Duncan, Abbott & Roberts, 1999)
Duncan, B., Abbott, S. & Roberts, R. (1999)
Measurement Good Practice Guide No. 26 - Adhesive Tack.
UK, Teddington, Middlesex, TW11 0LW, National Physical Laboratory. ISSN 1368-6550

(Enrione, Hill & Mitchell, 2007)
Enrione, J. I., Hill, S. E., & Mitchell, J. R. (2007)
Sorption and diffusional studies of extruded waxy maize starch-glycerol systems.
Starch-Stärke, 59(1), pp. 1-9.
https://doi.org/10.1002/star.200600557

(EUCAST, 2016)
EUCAST: The European Committee on Antimicrobial Susceptibility Testing, (2016)
Breakpoint Tables for Interpretation of MICs and Zone Diameters, (Version 6.0)
http://www.eucast.org

(European Commission, 2011).
European Commission, (2011, 14 January)
Regulation (EU) No 10/2011 on plastic materials and articles intended to come into contact with food.
Official Journal of the European Union, 10/2011.

(Ferrer, Pal & Hubbe, 2017)
Ferrer, A., Pal, L., Hubbe, M. (2017).
Nanocellulose in packaging: Advances in barrier layer technologies.
Industrial Crops and Products, 95, 574–582.
https://doi.org/10.1016/j.indcrop.2016.11.012

(Gómez-Estaca, López de Lacey, López-Caballero, Gómez-Guillén & Montero, 2010)
Gómez-Estaca, J., López de Lacey, A., López-Caballero, M.E., Gómez-Guillén, M.C. & Montero, P. (2010)
Biodegradable gelatin–chitosan films incorporated with essential oils as antimicrobial agents for fish preservation.
Food microbiology, 27(7), pp. 889–896.
https://doi.org/10.1016/j.fm.2010.05.012.

(Gontard, Guilbert & Cuq, 1993)
Gontard, N., Guilbert, S., & Cuq, J. L. (1993)
Water and glycerol as plasticizers affect mechanical and water vapor barrier properties of an edible wheat gluten film.
Journal of food science, 58(1), pp. 206-211.
https://doi.org/10.1111/j.1365-2621.1993.tb03246.x

(Guo, Ge, Li, Mu & Li, 2014)
Guo, J., Ge, L., Li, X., Mu, C., & Li, D. (2014).
Periodate oxidation of xanthan gum and its crosslinking effects on gelatin-based edible films. Food Hydrocolloids, 39, pp. 243–250.
https://doi.org/10.1016/j.foodhyd.2014.01.026

(Guo et al., 2019)
Guo, T., Gu, L., Zhang, Y., Chen, H., Jiang, B., Zhao, H., Jin, Y. & Xiao H. (2019)
Bioinspired self-assembled films of carboxymethyl cellulose–dopamine/montmorillonite
Journal of Material Chemistry A,7, pp. 14033-14041
https://doi.org/10.1039/C9TA00998A

(Haghighi et al., 2019a)
Haghighi, H., De Leo, R., Bedin, E., Pfeifer, F., Siesler, H. W. & Pulvirenti, A. (2019)

Comparative analysis of blend and bilayer films based on chitosan and gelatin enriched with LAE (lauroylarginate ethyl) with antimicrobial activity for food packaging applications.
Food Packaging and Shelf Life, 19, pp. 31-39.
https://doi.org/10.1016/j.fpsl.2018.11.015

(Haghighi et al., 2019b)
Haghighi, H., Biard, S., Bigi, F., De Leo, R., Bedin, E., Pfeifer, F., Siesler, H. W., Licciardello, F. & Pulvirenti, A. (2019)
Comprehensive characterization of active chitosan-gelatin blend films enriched with different essential oils.
Food Hydrocolloids 95 (2019) 33–42
http://dx.doi.org/10.1016/j.foodhyd.2019.04.019

(Hamaguchi, WuYin & Tanaka, 2007)
Hamaguchi, P. Y., WuYin, W., & Tanaka, M. (2007)
Effect of pH on the formation of edible films made from the muscle proteins of Blue marlin (Makairamazara).
Food Chemistry, 100(3), pp. 914-920.
https://doi.org/10.1016/j.foodchem.2005.10.045

(Hasheminya, Mokarram, Ghanbarzadeh, Hamishekar & Kafil, 2018)
Hasheminya, S. M., Mokarram, R. R., Ghanbarzadeh, B., Hamishekar, H., & Kafil, H. S. (2018).
Physicochemical, mechanical, optical, microstructural and antimicrobial properties of novel kefiran-carboxymethyl cellulose biocomposite films as influenced by copper oxide nanoparticles (CuO-NPs).
Food Packaging and Shelf Life, 17, 196–204.
Hhttps://doi.org/10.1016/j.fpsl.2018.07.003

(He, Fei & Li, 2019)
He, Y., Fei, X., Li, H. (2019)
Carboxymethyl cellulose-based nanocomposites reinforced with montmorillonite and ε-poly-L-lysine for antimicrobial active food packaging.
Journal of Applied Polymer Science 137(23), 48782.
https://doi.org/10.1002/app.48782

(Hosseini, Rezaei, Zandi & Farahmandghavi, 2015)
Hosseini, S. F., Rezaei, M., Zandi, M. & Farahmandghavi, F. (2015)
Fabrication of bio-nanocomposite films based on fish gelatin reinforced with chitosan nanoparticles.
Food Hydrocolloids, 44, pp. 172-182.
https://doi.org/10.1016/j.foodhyd.2014.09.004

(Kamide et al., 1985)
Kamide, K., Okajima, K., Kowsaka, K., Matsui, T., Nomura, S., & Hikichi, K. (1985)
Effect of the distribution of substitution of the sodium salt of carboxymethylcellulose on its absorbency toward aqueous liquid.
Polymer journal, 17(8), pp. 909-918.

https://doi.org/10.1295/polymj.17.909

(Kanatt & Makwana, 2020)
Kanatt, S. R. & Makwana, S. H. (2020)
Development of active, water-resistant carboxymethyl cellulose-poly vinyl alcohol-Aloe vera packaging film.
Carbohydrate Polymers, 227, 115303.
https://doi.org/10.1016/j.carbpol.2019.115303

(Kim, Lee & Park, 1995)
Kim, Y.J., Lee, H.M., Park, O.O. (1995)
Processabilities and mechanical properties of Surlyn-treated starch/LDPE blends.
Polymer Engineering and Science, 35, pp. 1652-1657
https://doi.org/10.1002/pen.760352012

(Lee, Yam & Piergiovanni, 2008)
Lee, D.S., Yam, K.L., Piergiovanni, L. (2008).
Food Packaging Science and Technology.
New York: CRC Press, Boca Raton, pp. 243–274.
https://doi.org/10.1201/9781439894071

(Liu, Song, Shang, Song & Wang, 2012)
Liu, H., Song, J., Shang, S., Song, Z., Wang, D. (2012)
Cellulose nanocrystal/silver nanoparticle composites as bifunctional nanofillers within waterborne polyurethane.
ACS Applied Materials & Interfaces, 4(5), 2413-9.
https://doi.org/10.1021/am3000209

(Marsh & Bugusu, 2007)
Marsh, K. & Bugusu, B. (2007)
Food Packaging—Roles, Materials, and Environmental Issues.
Journal of Food Science, 72(3), pp. 39-55.
https://doi.org/10.1111/j.1750-3841.2007.00301.x

(Moghimi, Aliahmadi & Rafati, 2017)
Moghimi, R., Aliahmadi, A. & Rafati, H. (2017)
Antibacterial hydroxypropyl methyl cellulose edible films containing nanoemulsions of Thymus daenensis essential oil for food packaging.
Carbohydrate Polymers, 175, pp. 241-248.
https://doi.org/10.1016/j.carbpol.2017.07.086

(Muppalla, Kanatt, Chawla & Sharma, 2014)
Muppalla, S. R., Kanatt, S. R., Chawla, S.P. & Sharma. A. (2014)
Carboxymethyl cellulose–polyvinyl alcohol films with clove oil for active packaging of ground chicken meat.
Food Packagng and Shelf Life, 2, pp. 51-58.
https://dx.doi.org/10.1016/j.fpsl.2014.07.002

(Nur Hazirah, Isa, Sarbon, 2016)
Nur Hazirah, M.A.S.P., Isa, M.I.N., Sarbon, N.M. (2016)
Effect of xanthan gum on the physical and mechanical properties of gelatin-carboxymethyl cellulose film blends
Food Packaging and Shelf Life, 9, 55–63

(O'sullivan, 1997)
O'sullivan, A. C. (1997)
Cellulose: the structure slowly unravels.
Cellulose, 4(3), pp. 173-207.
https://doi.org/10.1023/A:1018431705579

(Pérez & Mazeau, 2005)
Pérez, S. & Mazeau, K. (2005)
Conformations, structures, and morphologies of celluloses.
In S. Dumitriu (Ed), Polysaccharides: Structural diversity and functional versatility (2nd edition)
Marcel Dekker: New York
https://doi.org/10.1021/ja0410486

(Quintavalla & Vicini, 2002)
Quintavalla, S. & Vicini, L. (2002)
Antimicrobial food packaging in meat industry.
Meat science, 62(3), pp. 373–380. https://doi.org/10.1016/s0309-1740(02)00121-3

(Qiu, Shaoa, Liuc, Wanga, Lic & Zhao 2014).
Qiu, L., Shaoa,Z., Liuc, M., Wanga, J., Lic, P. & Zhao, M. (2014).
Synthesis and electrospinning carboxymethyl cellulose lithium(CMC-Li) modified 9,10-anthraquinone (AQ) high-ratelithium-ion battery.
Carbohydrate Polymers 102, 986– 992
http://dx.doi.org/10.1016/j.carbpol.2013.09.105

(Siracusa, Rocculi, Romani & Rosa, 2008)
Siracusa, V., Rocculi, P., Romani, S., & Rosa, M. D. (2008)
Biodegradable polymers for food packaging: A review.
Trends in Food Science & Technology, 19(12), pp. 634–643.
https://doi.org/10.1016/j.tifs.2008.07.003.

(Shyu, Chen, Chiang & Sung, 2008)
Shyu, Y.-S., Chen, G.-W., Chiang S.-C. & Sung W.-C., (2008)
Effect of Chitosan and Fish Gelatin Coatings on Preventing the Deterioration and Preserving the Quality of Fresh-Cut Apples
Molecules, 24.
doi:10.3390/molecules24102008

(Su, Huang, Yuan, Wang & Li, 2010)
Su, J. F., Huang, Z., Yuan, X. Y., Wang, X. Y., & Li, M. (2010)

Structure and properties of carboxymethyl cellulose/soy protein isolate blend edible films crosslinked by Maillard reactions.
Carbohydrate polymers, 79(1), pp. 145-153
https://doi.org/10.1016/j.carbpol.2009.07.035

(Sunardi, & Ahmad 2017)
Sunardi, N. M. F. & Ahmad B.J. (2017)
Preparation of carboxymethyl cellulose produced from purun tikus (Eleocharis dulcis)
AIP Conference Proceedings 1868, 020008 (2017)
https://doi.org/10.1063/1.4995094

(Theerawitayaart, Prodpran, Benjakul, and Sookchoo, 2019)
Theerawitayaart, W., Prodpran, T., Benjakul, S., Sookchoo, P. (2019)
Properties of films from fish gelatin prepared by molecular modification and direct addition of oxidized linoleic acid.
Food Hydrocolloids, 88, 291–300
https://doi.org/10.1016/j.foodhyd.2018.10.022

(Tong, Xiao & Lim, 2008)
Tong, Q., Xiao, Q. & Lim, L-T. (2008)
Preparation and properties of pullulan–alginate–carboxymethylcellulose blend films.
Food Research International 41 (2008) 1007–1014
https://doi.org/10.1016/j.foodres.2008.08.005Get rights and content

(Villalobos, Hernández-Muñoz & Chiralt, 2006)
Villalobos, R., Hernández-Muñoz, P., & Chiralt, A. (2006)
Effect of surfactants on water sorption and barrier properties of hydroxypropyl methylcellulose films.
Food Hydrocolloids, 20(4), pp. 502-509.
https://doi.org/10.1016/j.foodhyd.2005.04.006

(Wrona, Cranb, Nerín & Bigger, 2017)
Wrona, M., Cranb, M. J., Nerín, C., Bigger, S. W. (2017)
Development and characterization of HPMC films containing PLA nanoparticles loaded with green tea extract for food packaging applications.
Carbohydrate Polymers 156, 108–117.
https://doi.org/10.1016/j.carbpol.2016.08.094.

(Wu, Sun, Guo, Ge & Zhang, 2017)
Wu, J., Sun, X., Guo, X., Ge, S. & Zhang, Q. (2017).
Physicochemical properties, anti- microbial activity and oil release of fish gelatin films ncorporated with cinnamon essential oil.
Aquaculture and Fisheries, 2(4), 185–192.
https://doi.org/10.1016/j.aaf. 2017.06.004

(Zeman & Kubìk, 2007)

Zeman, S. & Kubìk, L. (2007)
Permeability of polymeric packaging materials.
Technical Science, 10
https://doi.org/10.2478/v10022-007-0004-6

(Zhao, Lyu, Lee, Cui, & Chem, 2019)
Zhao, G., Lyu, X., Lee, J., Cui, X. & Chem, W-N. (2019)
Biodegradable and transparent cellulose film prepared eco-friendly from durian rind for packaging application.
Food Packaging and Shelf Life, 21, 100345.
https://doi.org/10.1016/j.fpsl.2019.100345

(Zhao, Wei, Xu & Han, 2020)
Zhao, J., Wei, F., Xu, W. & Han, X. (2020)
Enhanced antibacterial performance of gelatin\chitosan film containing capsaicin loaded MOFs for food packaging.
Applied Surface Science, 510, 145418
https://doi.org/10.1016/j.apsusc.2020.145418

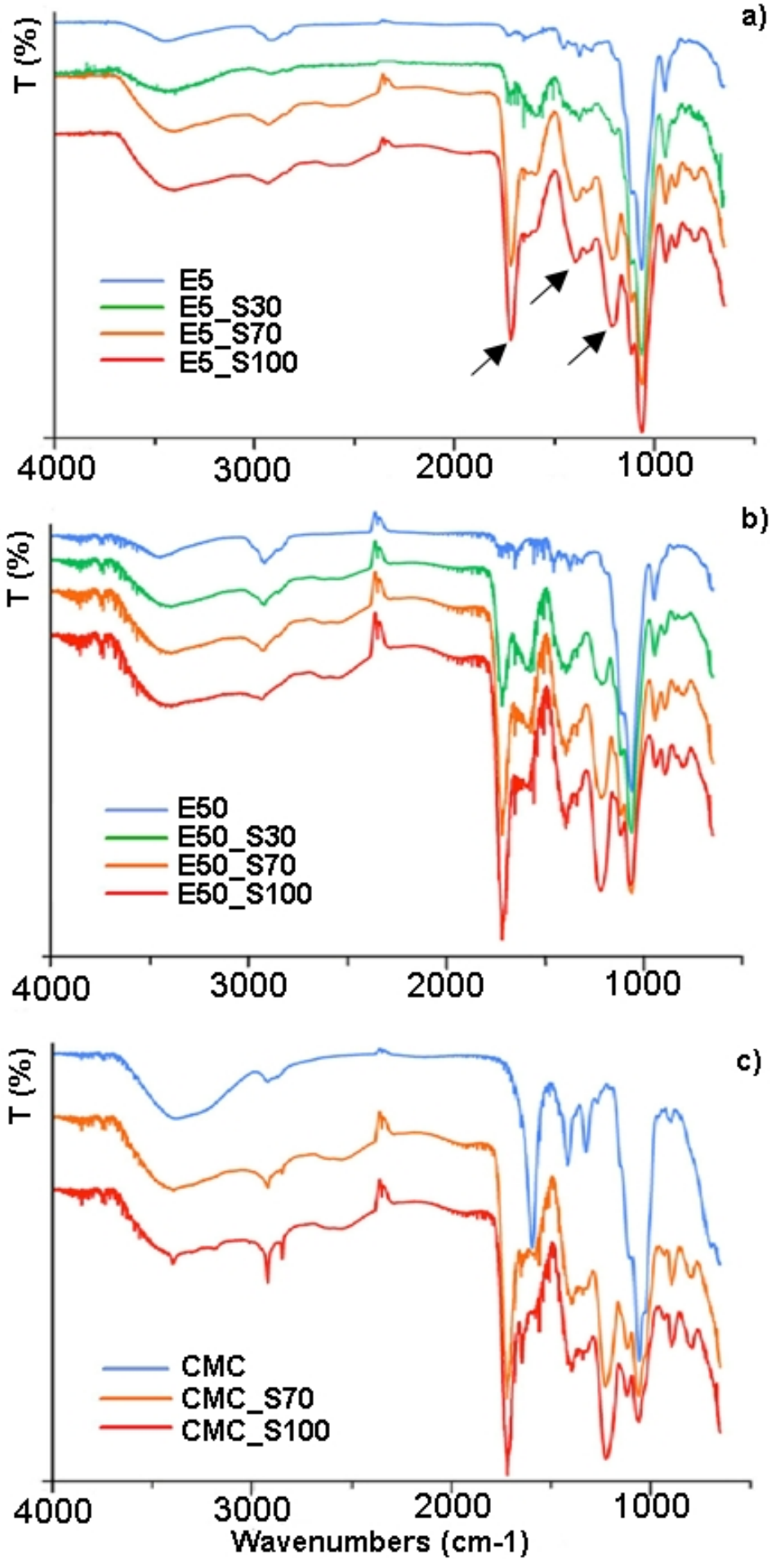
a)
T (%)
E5
E5_S30
E5_S70
E5_S100
4000
3000
2000
1000
b)
T (%)
E50
E50_S30
E50_S70
E50_S100
4000
3000
2000
1000
c)
T (%)
CMC
CMC_S70
CMC_S100
4000
3000
2000
1000
Wavenumbers (cm-1)

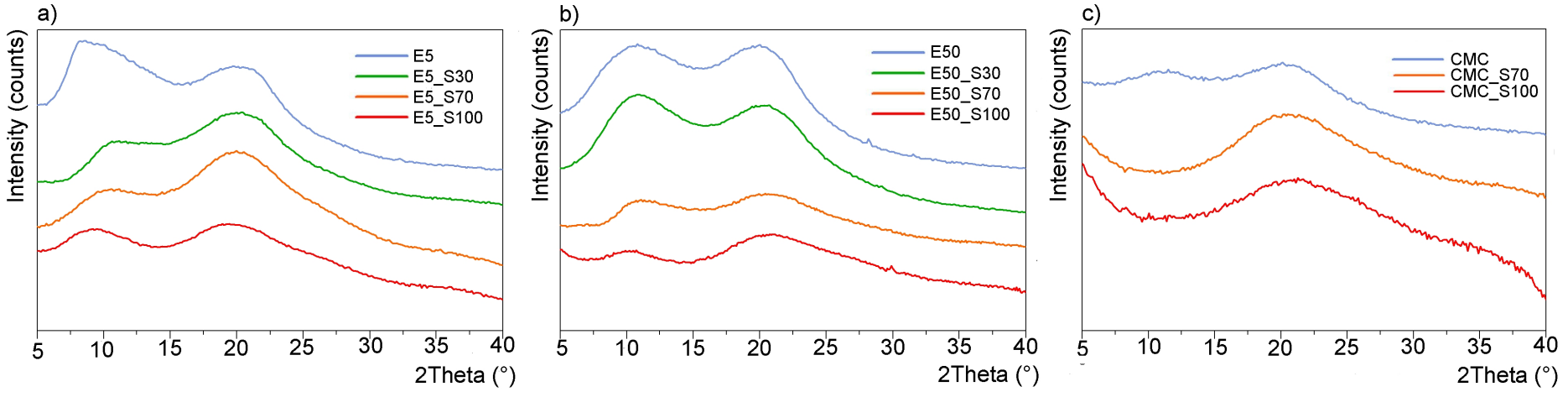
a)
Intensity (counts)
E5
E5_S30
E5_S70
E5_S100
5
10
15
20
25
30
35
40
2Theta (°)
b)
Intensity (counts)
E50
E50_S30
E50_S70
E50_S100
5
10
15
20
25
30
35
40
2Theta (°)
c)
Intensity (counts)
CMC
CMC_S70
CMC_S100
5
10
15
20
25
30
35
40
2Theta (°)

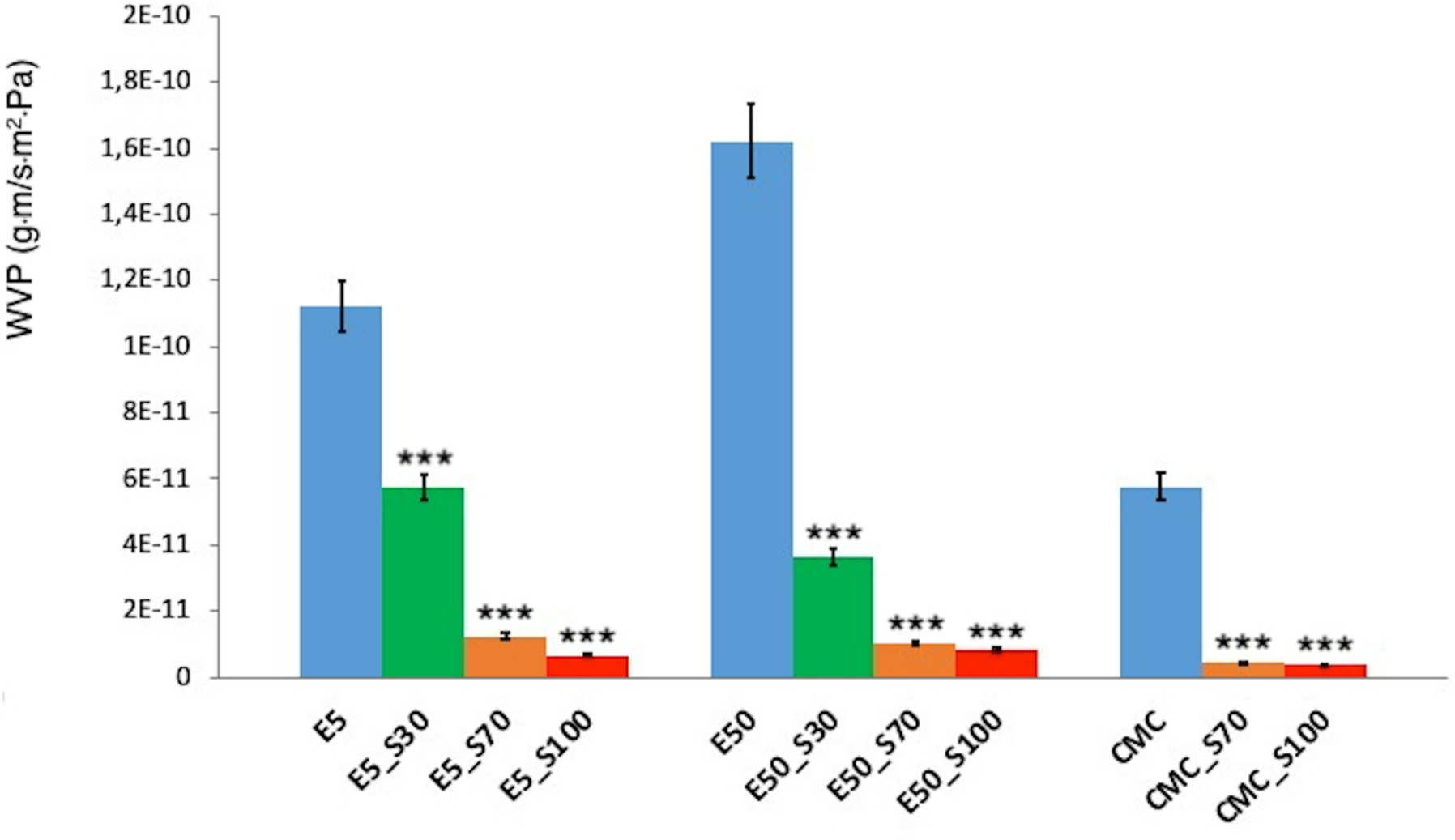
WVP (g·m/s·m²·Pa)
2E-10
1,8E-10
1,6E-10
1,4E-10
1,2E-10
1E-10
8E-11
6E-11
4E-11
2E-11
0
***
E5
E5_S30
E5_S70
E5_S100
E50
E50_S30
E50_S70
E50_S100
CMC
CMC_S70
CMC_S100

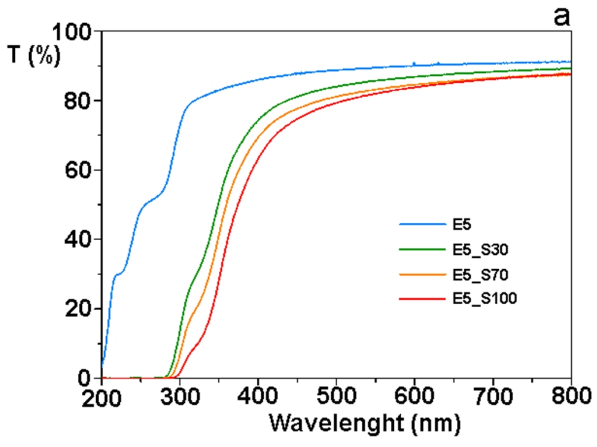
a
T (%)
100
80
60
40
20
0
200
300
400
500
600
700
800
Wavelenght (nm)
E5
E5_S30
E5_S70
E5_S100

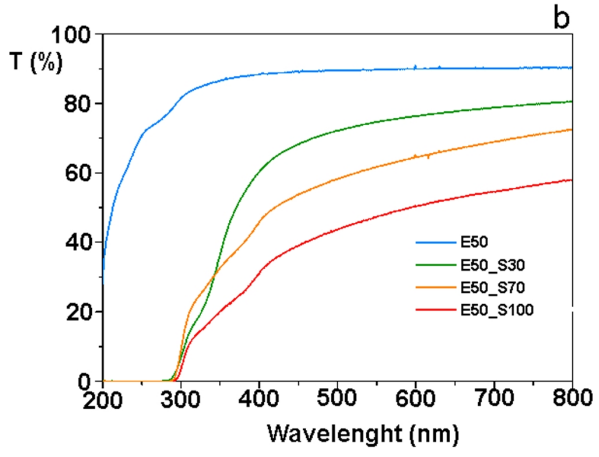
b
T (%)
100
80
60
40
20
0
200
300
400
500
600
700
800
Wavelenght (nm)
E50
E50_S30
E50_S70
E50_S100

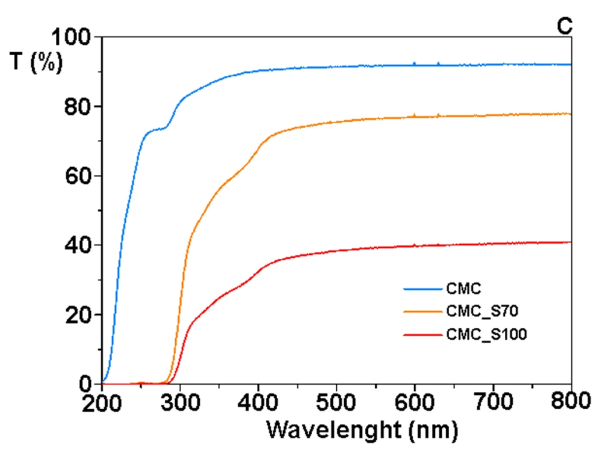
c
T (%)
100
80
60
40
20
0
200
300
400
500
600
700
800
Wavelenght (nm)
CMC
CMC_S70
CMC_S100

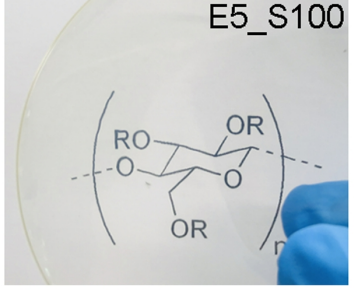
E5_S100
RO
OR
O
O
OR
n

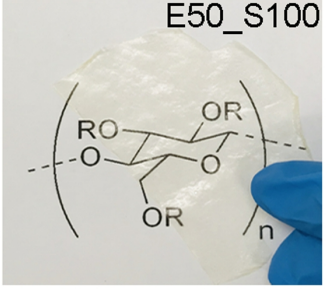
E50_S100
RO
OR
O
O
OR
n

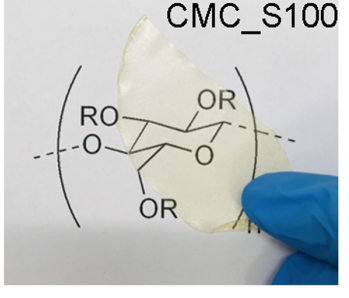
CMC_S100
RO
OR
O
O
OR

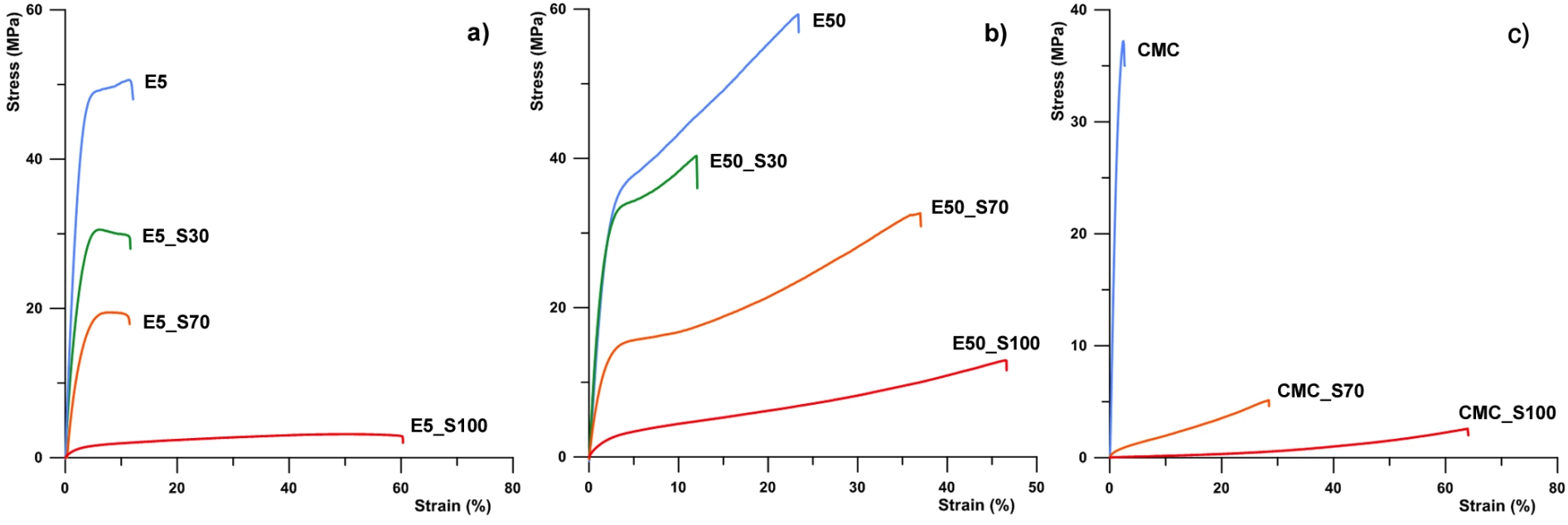
a)
Stress (MPa)
Strain (%)
E5
E5_S30
E5_S70
E5_S100
b)
E50
E50_S30
E50_S70
E50_S100
c)
CMC
CMC_S70
CMC_S100

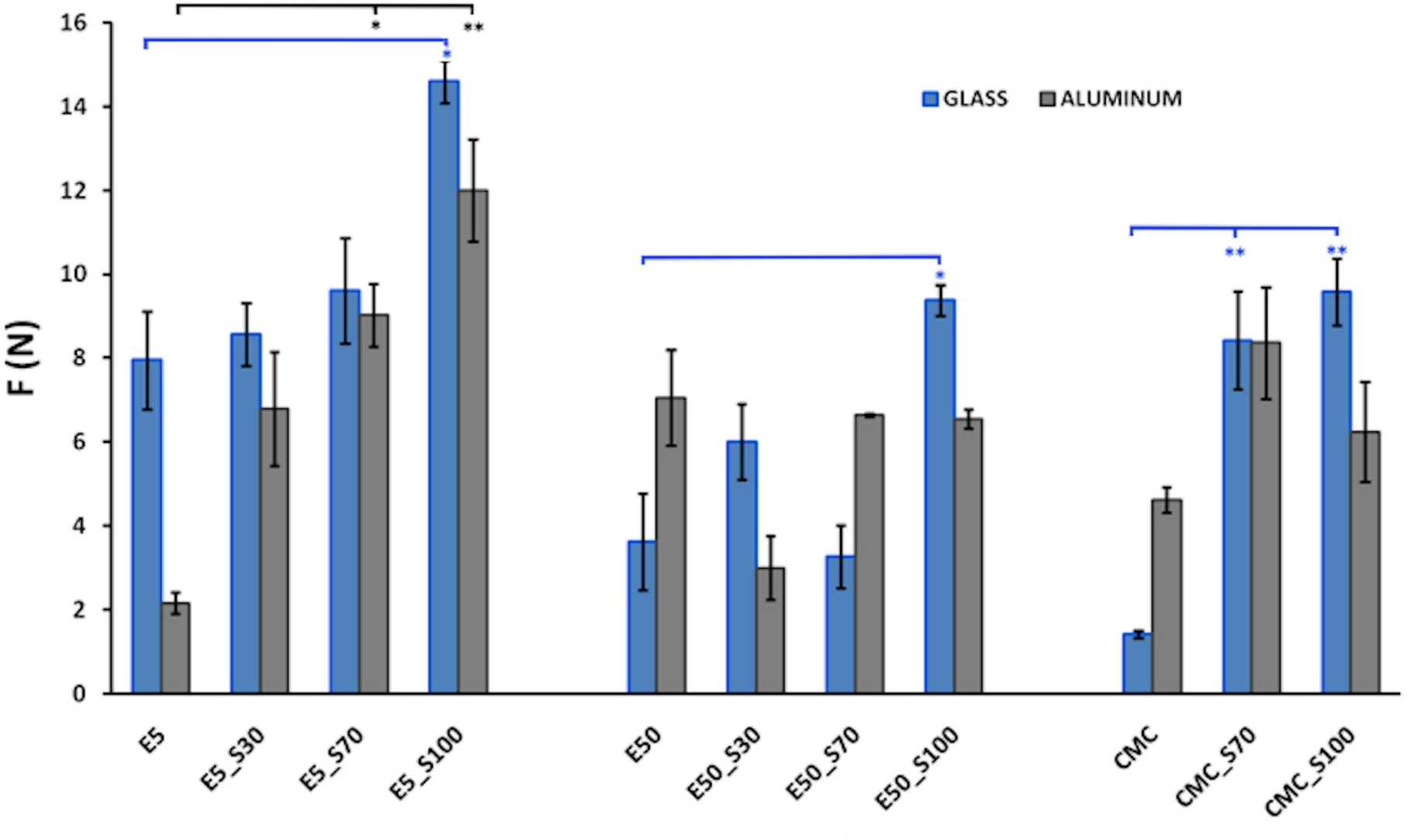
F (N)
16
14
12
10
8
6
4
2
0
GLASS
ALUMINUM
*
**
*
*
**
**
E5
E5_S30
E5_S70
E5_S100
E50
E50_S30
E50_S70
E50_S100
CMC
CMC_S70
CMC_S100

t = 0

t = 10 days

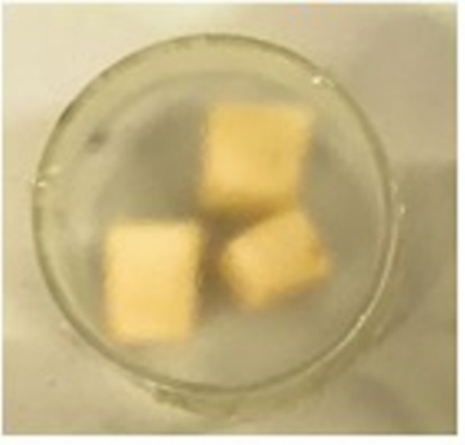

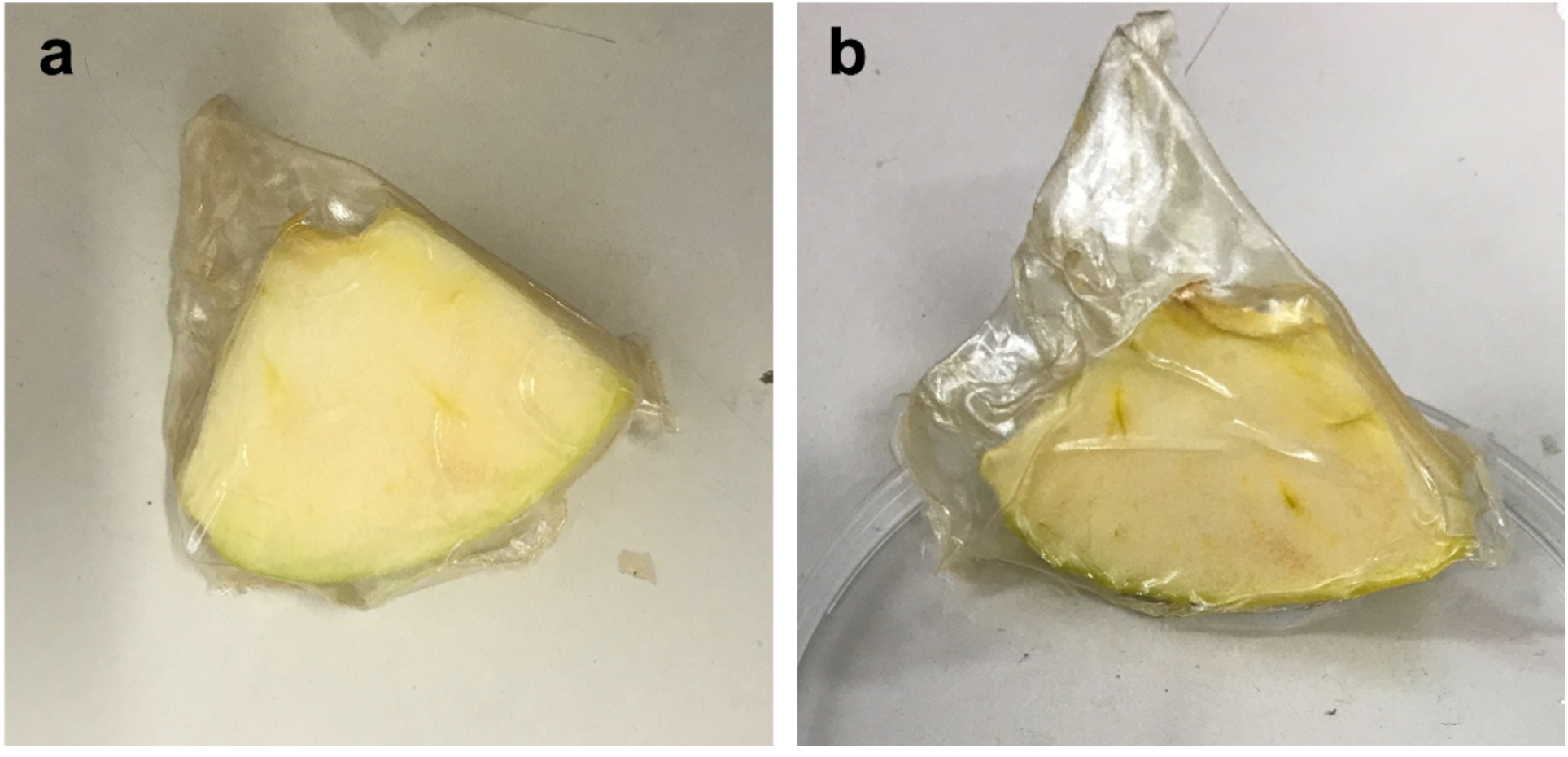
a
b

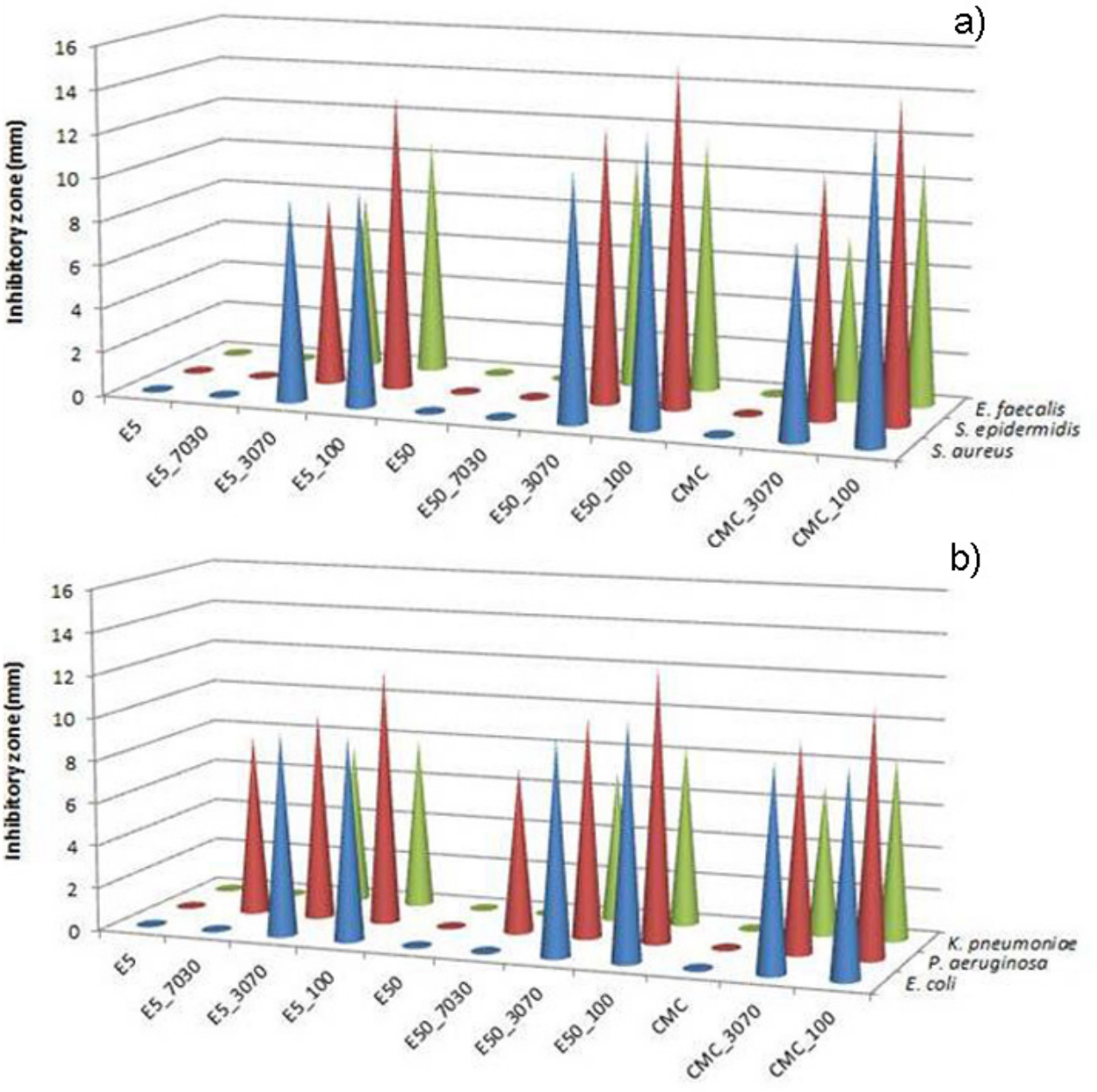
a)
Inhibitory zone (mm)
16
14
12
10
8
6
4
2
0
E5
E5_7030
E5_3070
E5_100
E50
E50_7030
E50_3070
E50_100
CMC
CMC_3070
CMC_100
E. faecalis
S. epidermidis
S. aureus
b)
Inhibitory zone (mm)
16
14
12
10
8
6
4
2
0
E5
E5_7030
E5_3070
E5_100
E50
E50_7030
E50_3070
E50_100
CMC
CMC_3070
CMC_100
K. pneumoniae
P. aeruginosa
E. coli

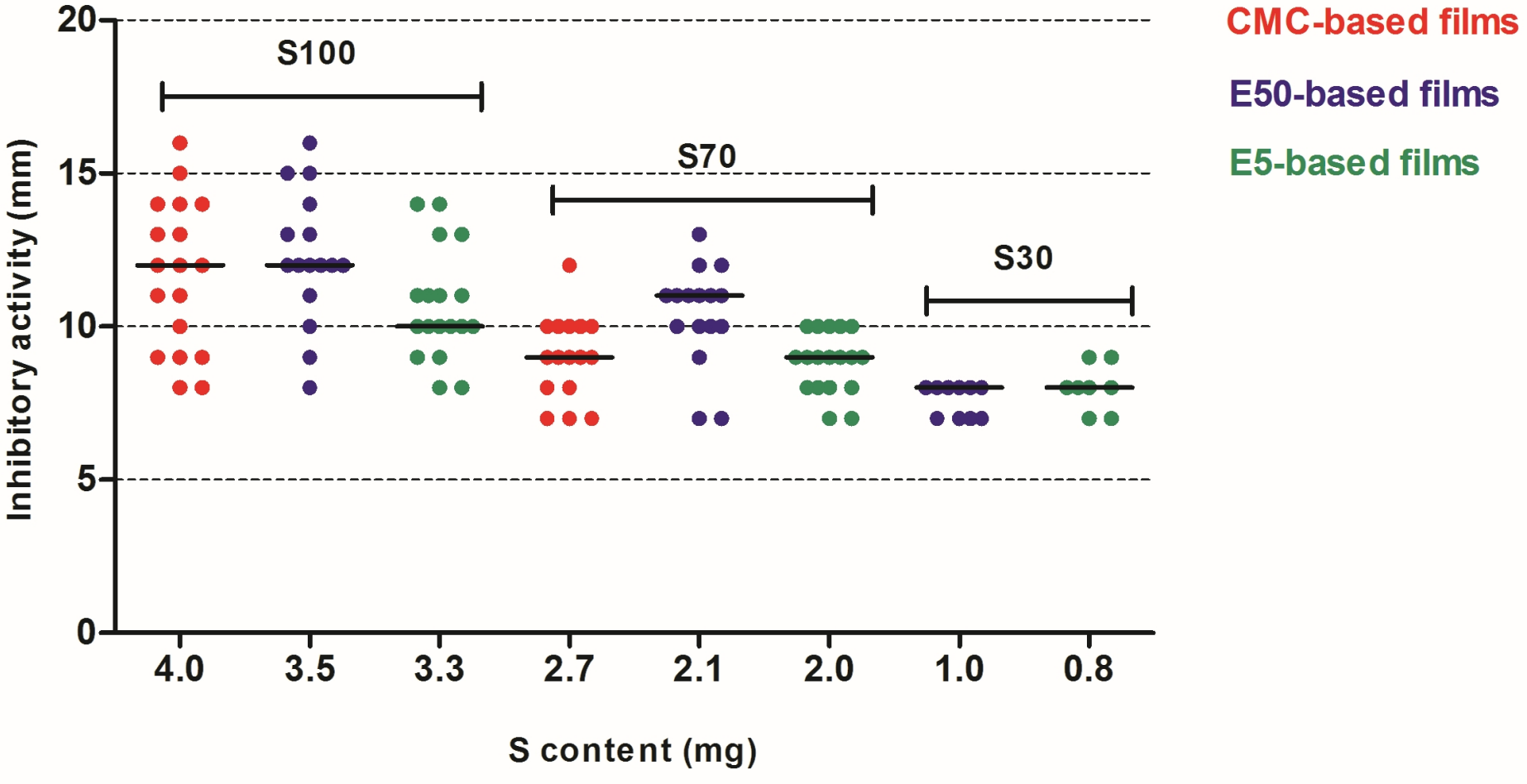
CMC-based films
E50-based films
E5-based films
S100
S70
S30
Inhibitory activity (mm)
20
15
10
5
0
4.0
3.5
3.3
2.7
2.1
2.0
1.0
0.8
S content (mg)

Declaration of competing interest

The authors declare that they have no conflict of interest in the publication of this manuscript. This study is original research that has not been published previously, and not under consideration for publication elsewhere.

CRediT authorship contribution statement

Maria Francesca di Filippo: Conceptualization, Methodology, Writing - original draft

Luisa stella Dolci: Conceptualization, Methodology, Writing - original draft

Letizia Liccardo: Data curation, Formal analysis, Writing - original draft

Silvia Panzavolta: Supervision, Data curation, Writing - review & editing.

Beatrice Albertini: Data curation, Writing - review & editing.

Nadia Passerini: Validation, Resources

Giovanna Angela Gentilomi: Validation Francesca Bonvicini: Data curation, Investigation

Adriana Bigi: Resources, Review.

CELLULOSE DERIVATIVES-SNAIL SLIME FILMS: NEW DISPOSABLE ECO-FRIENDLY MATERIALS FOR FOOD PACKAGING

Maria Francesca Di Filippo[1 §], Luisa Stella Dolci[2 §], Letizia Liccardo[1], Adriana Bigi[1], Francesca Bonvicini[3], Giovanna Angela Gentilomi[3], Nadia Passerini[2], Silvia Panzavolta[1*], Beatrice Albertini[2]

[1]Department of Chemistry "G. Ciamician", University of Bologna, Via Selmi 2, 40126, Italy;

[2]Department of Pharmacy and BioTechnology, University of Bologna, Via S. Donato 19/2, 40127, Italy;

[3]Department of Pharmacy and Biotechnology, University of Bologna, Via Massarenti 9, 40138, Italy

§ these Authors equally contributed to this work

*Corresponding author: Silvia Panzavolta

Table S1: composition of Snail mucus extract as reported by the producer

Specification	Values	Measure Units	Method
Aspect	Clear		
smell	Odorless		
Color	Pale yellow		
pH	2.9		
Density	1.0-1.04	g/ml	
Dry residual	5 %	M/V	M.I.M 180305/L Rev. 0:2005
Minerals (K, Ca, Na)	538	mg/L	M.I.M 110315/C Rev. 0:2005
Heavy metals	absent		
Proteins	80 - 120	mg/L	Bradford proteins assay method
Glycolic acid	60-80	mg/L	J. Chrom. A. 1322, pp 49-53, 2013
Allantoin	100-130	mg/L	J. Chrom. A. 1322, pp 49-53, 2013
Iron	3	mg/L	M.I.M 111010/C Rev. 0:2010
Citric acid	<0.1	mg/L	M.I.M 150212/A Rev. 0:2012
Ascorbic acid	<0.1	mg/L	M.I.M 150212/A Rev. 0:2012
Antiprotease	1.3	mg/L	M.I.M 0112016/A Rev. 0:2016
D-lactic Acid	<10	mg/L	M.I.M 0112016/A Rev. 0
L-lactic Acid	<10	mg/L	M.I.M 0112016/A Rev. 0
Sodium benzoate	<0.002%	m/m	M.I.M 150212/A Rev 0:2012
Collagen	2-60	mg/L	M.I.M 0112016/H Rev. 0:2016
Gram +	<10	UFC/g	UNI-EN ISO6888-1:2004
Gram -	<10	UFC/g	ISO 16649-2:2001
Fungi	<10	UFC/g	NFV08-059:2002

Figure S1. Chemical structure of: left) hydroxypropyl methylcellulose and right) carboxymethyl cellulose and their characteristics.

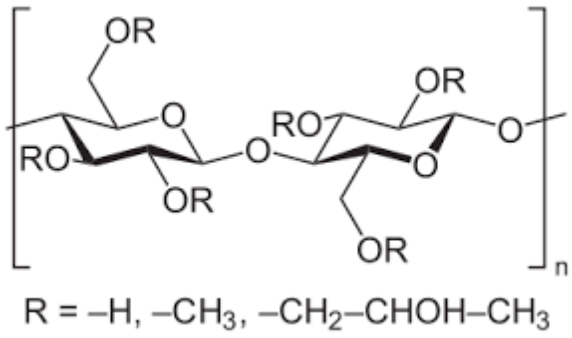

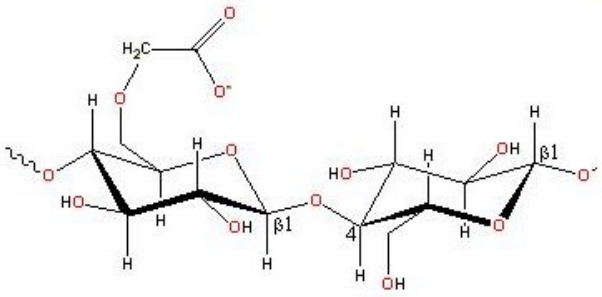

Product Description	**METHOCEL E5**	**METHOCEL E50**	**CMCNa**
Methoxyl, %	28-30	28-30	--
Hydroxypropyl, %	7-12	7-12	--
Viscosity, 2% in water, mPa•s	4-6	40-60	850

Figure S2: Infrared spectrum of lyophilized Snail extract.

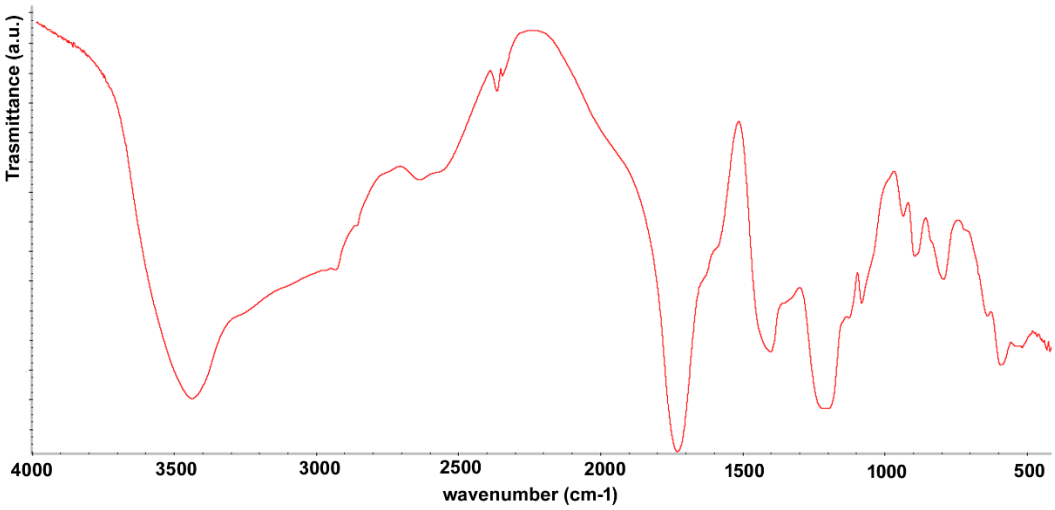

Figure S3: Moisture sorption isotherms of E5-based films (a) and CMC-based films (b).